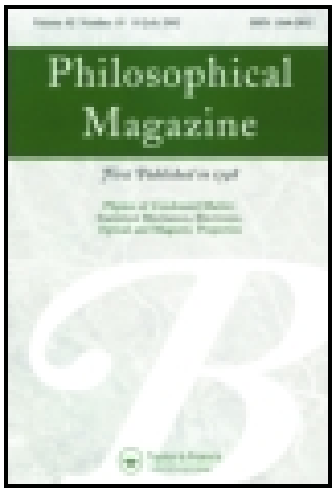

Philosophical Magazine Part B
Publication details, including instructions for authors and subscription information:
http://www.tandfonline.com/loi/tphb20

The explosive disintegration of Prince Rupert's drops

S. Chandrasekar [a b] & M. M. Chaudhri [a]
[a] Cavendish Laboratory , Cambridge University , Madingley Road, Cambridge, CB3 OHE, England
[b] Schools of Engineering, Purdue University , West Lafayette, IN, 47907, USA
Published online: 27 Sep 2006.

To cite this article: S. Chandrasekar & M. M. Chaudhri (1994) The explosive disintegration of Prince Rupert's drops, Philosophical Magazine Part B, 70:6, 1195-1218, DOI: 10.1080/01418639408240284

To link to this article: http://dx.doi.org/10.1080/01418639408240284

PHILOSOPHICAL MAGAZINE B, 1994, VOL. 70, NO. 6, 1195–1218

The explosive disintegration of Prince Rupert's drops

By S. CHANDRASEKAR† and M. M. CHAUDHRI

Cavendish Laboratory, Cambridge University, Madingley Road, Cambridge CB3 0HE, England

[*Received 14 February 1994‡ and accepted 21 May 1994*]

ABSTRACT

A high-speed photographic study has been made of the explosive disintegration of Prince Rupert's drops. The drops were prepared by quenching molten soda-lime glass in water. The disintegration of a drop was initiated by exploding a small (26 mg) lead azide charge or by impacting with a hardened steel chisel on to the tail of the drop. The entire fragmentation process was recorded at framing rates ranging from 6500 frames s^{-1} to $0{\cdot}5 \times 10^6 s^{-1}$. The high-speed photographic sequences revealed that in a disintegrating drop the crack front, having been initiated in the tail, propagated at a high velocity ($\approx$ 1450–1900 ms^{-1}) within the tensile zone, towards the drop's head. Finger-type bifurcating cracks at the crack front were observed. High-speed photographic observations, combined with an analysis of the fragment sizes, indicated that the fast-moving cracks slowed down dramatically on entering the surface compression zone. Sequences of high-speed shadowgraphs also revealed that the rapidly moving crack front did not produce any strong stress waves in the drops which could have contributed to their explosive disintegration. The main features of crack propagation in a drop were found to be similar to those of the self-propagating cracks in thermally tempered soda-lime glass blocks. Measurements of residual stresses in the drops using an indentation technique showed that the surface compressive stress was $\approx$ 90–170 MPa and the tension zone extended across $\approx$ 70% of the drop's diameter at the head. Both of these values are similar to those found for thermally tempered soda-lime glass blocks. A model based on the repeated bifurcation of fast-moving cracks within the tensile zone in the drop has been proposed to explain its explosive disintegration.

§ 1. INTRODUCTION

Special 'glass bubbles' (now referred to as Prince Rupert's drops) possessing some very striking mechanical properties appear to have been in existence since before 1625 in Mecklenburg (Brodsley, Frank and Steeds 1986). They were also known as Batavian drops and Prince Rupert of Bavaria is said to have been the first to bring them from Germany to England (Merrett 1662, Peligot 1877). King Charles II communicated them to his Society (later to be called the Royal Society) at Gresham College, London in 1660–1661, and sought an explanation for their physical nature from the Society. A transcribed account of the Society's findings by Sir Robert Moray in 1661 was first reported by Merrett (1662). Since then, numerous investigations of the properties of these drops have been made, especially during the seventeenth century, and Brodsley

† Permanent address: Schools of Engineering, Purdue University, West Lafayette, IN 47907, USA.

‡ Received in final form 27 April 1994.

Fig. 1

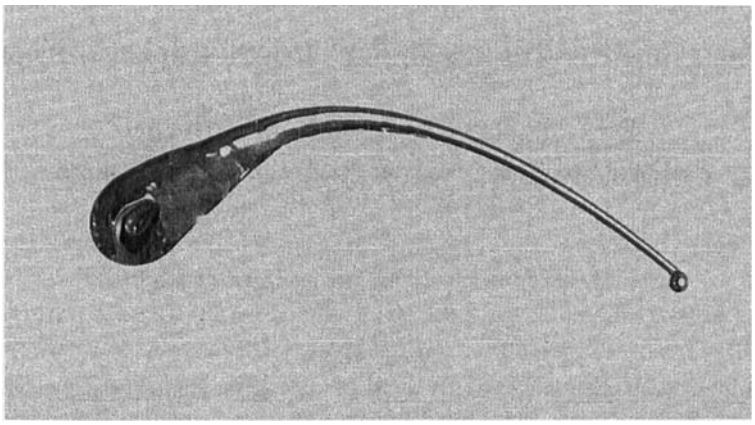

Photograph of a typical tadpole-shaped Prince Rupert's drop made of soda-lime glass. The small sphere at the end of the tail formed when the tail was detached from the parent glass rod using a gas flame.

et al. (1986) have given a detailed and informative review of the literary, historical and scientific aspects of the subject.

Prince Rupert's drops are tadpole-shaped drops of solidified flint or soda-lime glass and they usually have fine extended tails (see fig. 1). Nowadays such drops are formed by allowing molten glass from the end of a heated glass rod to fall into cold water, which cools down the surface layers very rapidly. The drops produced in this manner are generally found to have voids or bubbles in their interior, though drops without voids can also be formed. These voids are now thought to contain vacuoles (Brodsley *et al.* 1986), although Hooke (1665) had suggested that the voids contained some material which was dispersed within the bulk of the glass. In the present-day terminology, one may think of this material as occluded gases.

Rupert's drops show very perplexing strength properties: the head of a drop will not break when it is hammered on an anvil. In fact, a drop having a head 6–8 mm in diameter could be pressed between two hardened steel rollers to loads of up to 15 000 N without breaking. However, when its tail is broken with a mild pressure applied with the finger, the entire drop will disintegrate within microseconds (see § 3) producing a fine powder. Hooke (1665) made an extensive investigation of the fracture behaviour of these drops using an optical microscope. He postulated that the rapid quenching of the drops in water left their interior in a state of tension, which was relieved by the process of catastrophic disintegration upon breaking its tail. To support this hypothesis, he thermally annealed the drops and showed that the annealed drops lost their ability to disintegrate catastrophically. Earlier, Moray (see Merrett (1662)) had reported the same.

About two centuries later, de Luynes (1873) put forward a hypothesis which was quite similar to that of Hooke (1665), though no reference to Hooke's work was made. de Luynes suggested that there were different degrees of tension in a Rupert's drop, with the maximum at the surface and the minimum at the centre of the drop. Peligot (1877) supported the hypothesis of de Luynes (1873) regarding the cause of the tension in a Rupert's drop and thought that its mechanical properties were closely related to those of thermally tempered glass invented by de la Bastie (1874), who believed that

the rapid quenching of glass hardened its surface in the same manner as that of quenched steel.

Contrary to the theories of Hooke (1665) and de Luynes (1875), it is now accepted that the surface of a Rupert's drop is in compression and the central zone in tension. However, it is not yet clear who first proposed this state of stress in a Rupert's drop. It appears that the stress distribution even in a block of thermally tempered glass was not clearly understood until the early part of the 20th century (see de Freminville (1914), Littleton and Preston (1929)). It seems, therefore, that once the stresses in tempered glass were understood, and because the process of formation of a Rupert's drop has many similarities with the tempering process, it became quite straightforward to assume a qualitative similarity of the compressive and tensile stresses in the Rupert's drop and in a block of thermally tempered glass.

Recently, Johnson and Chandrasekar (1992) calculated the solidification stresses, due to water quenching, in a tear-shaped (i.e., cone with a hemispherical head) soda-lime glass drop 6 mm in diameter at the head and 13 mm in length. They found that the surface compressive stresses were in the range of 50–80 MPa, while the tensile stresses at the drop's axis were in the range of 100–160 MPa. The calculated compressive stress values are similar to those present in commercially available thermally tempered soda-lime glass blocks.

Hooke (1665) also encased a few intact drops in transparent and tough glue with their tails remaining outside it. When the tail of an encased drop was broken, the entire drop fragmented but the fragments were preserved in position by the glue. His optical examination of the surface of the broken drop through the layer of glue indicated partial circumferential ring cracks, which did not form complete circles, as shown in fig. 2 (*a*). He thought that the fragments were parts of cone cracks, the apexes of which were towards the tail-end of the drop. He further thought that if he could make an axial section of a disintegrated drop, he would find the conical fragments arranged in a manner shown in fig. 2 (*b*). de Luynes (1873) carried out similar experiments on Rupert's drops encased in transparent glue. He drew sketches of the broken drops and thus supported Hooke's picture, though again no reference was made to his work. de Luynes (1873) found that the fragments were truncated cones with their apexes pointing towards the region where the process of disintegration was initiated, as shown in the various sketches given in fig. 3. de Luynes (1873) believed that because of the state of tension in the surface, the molecules of the glass there were stretched, and when a crack appeared on the surface the molecules contracted to their equilibrium lengths. Furthermore, since the tension was highest in the surface and insignificant at the centre of the drop, the contraction of the molecules was greatest on the surface and least at the centre. Such a picture would result in the formation of cones, with their apexes at the axis of the drop (see sketches in fig. 3).

We may note, however, that neither Hooke (1665) nor de Luynes (1873) proposed a mechanism for the progression of the disintegration from one conical fragment to the next. More recently, two hypotheses have been proposed to explain this disintegration phenomenon. Brodsley *et al.* (1986) suggested that 'if any of these is broken at some point, thus exposing its tensile core, a disintegration front propagates in both directions from that point with a speed similar to that of the transverse sound waves in glass, leaving behind a pattern of multiple fractures that divide the material into needle-like splinters ...'. They suggested that the propagation of the disintegration was helped by the release of the stored elastic energy in the drop, but did not propose a detailed mechanism. Regarding the high speed cracks, they referred to the third-year physics

Fig. 2

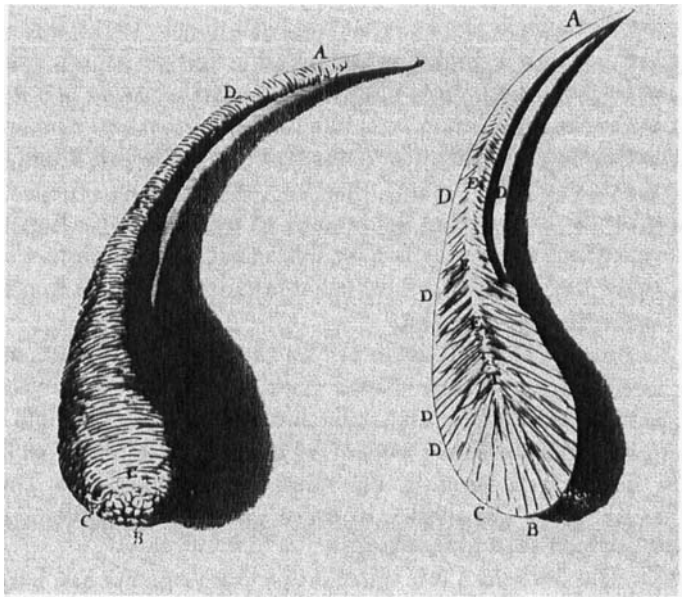

(*a*) (*b*)

Hooke's (1665) representations of disintegrated drops. (*a*) Shows the sketch of the circumferential ring cracks on the surface of a drop, which was encased in transparent glue before the disintegration; (*b*) is an imaginary axial section of a disintegrated drop. Note that both Brodsley *et al.* (1986) and Johnson and Chandrasekar (1992) incorrectly thought that this sectional view was actually observed by Hooke (1665).

undergraduate project theses of Harlin and Jones (1978). The second hypothesis for the disintegration of Rupert's drops proposed the initiation of new fracture sites in the head region of a drop due to the focusing of the stress waves generated by the disintegrating front travelling from the tail towards the head (Johnson and Chandrasekar 1992). We may add that neither of the two hypotheses has been supported by direct experimental evidence.

From what has been said in the above, it appeared to us that high-speed photographic observations of the dynamic crack propagation process in Rupert's drops during their explosive disintegration would help in resolving the disintegration mechanisms involved. Such a photographic technique has been extensively used to elucidate the dynamics of crack propagation in thermally tempered glass (Chaudhri and Liangyi 1986) and in ionic crystals (Chaudhri, Wells and Stephens 1981) when they were impacted with 1 and 2 mm diameter steel and tungsten carbide projectiles travelling at $\sim 150\,\mathrm{ms}^{-1}$.

Here we report the results from a high-speed photographic investigation (maximum framing rate: $0{\cdot}5 \times 10^6$ frames s^{-1}) of the disintegration of Prince Rupert's drops made of soda-lime glass. An important aspect of the work is that we were able to examine photographically the interior of the disintegrating drops. This study has enabled us to determine accurately the speed with which a disintegration front travels in a drop and the velocities of the fragments thus produced. Based on the photographic observations, a model for the propagation of disintegration is proposed.

Fig. 3

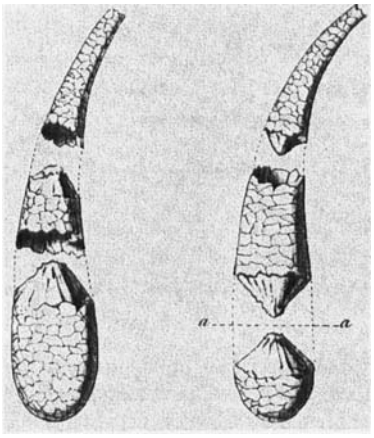

(*a*) (*b*)

Sketches of disintegrated Rupert's drops, which were encased in transparent glue when intact and then disintegrated by introducing in them fractures at different parts along their lengths (de Luynes 1873). In (*a*) the initiating crack was made in the tail and note that the apexes of the conical fragments are oriented towards the tail-end. In (*b*) the fracture was initiated at a point lying on the line aa. In this case one set of conical fragments, lying on one side of aa, has its apexes towards the tail, whereas the other set of fragments, lying on the other side of aa, has its apexes oriented towards the drop's head. Note also that the representations of the surfaces of disintegrated drops by Hooke (1665) and by de Luynes (1873) are different from each other in the sense that Hooke (1665) shows partial circumferential ring cracks, whereas de Luynes (1873) shows interconnected fragments.

§ 2. Experimental

Rupert's drops were made in the laboratory from soda-lime glass rods 5 and 7 mm in diameter. The composition of the soda-lime glass by weight was: SiO_2, 69%; B_2O_3, 1%; Na_2O, 13%; K_2O, 3%; Al_2O_3, 4%; BaO, 2%; CaO, 5%; MgO, 3%. The glass had a density of $2{\cdot}483 \times 10^3$ kg m^{-3}, refractive index of 1·523 for a wavelength of 435 nm, a Vickers hardness of 515 kgf mm^{-2} (indenter load 200 gf) and a fracture toughness K_{IC} of 0·75 MPa m$^{1/2}$. The drops were prepared by melting an end of a glass rod and allowing the molten glass to drop into a large glass beaker (150 mm in diameter) full of water kept at a temperature of 20°C. The tip of the melting end of the rod was kept at a distance of 375 mm from the surface of the water in the beaker. A piece of cardboard was placed at the bottom of the beaker to prevent the falling drop from coming into direct contact with the bottom glass surface of the beaker, thereby moderating the impact. (In spite of this precaution, some of the molten glass drops disintegrated while being cooled in the water. This disintegration was possibly due to any transient tensile stresses that developed at the surface of the drops during cooling.) Typically, the resulting glass drops resembled a tadpole in shape. The diameters of the hemispherical heads were in the range 5–14 mm, the tail diameters were approximately 0·2–0·5 mm, and the lengths of the tails were in the range 15–40 mm. Some of the drops had relatively straight tails while others had curved tails. Almost always the drops contained at least two or three bubbles within their head regions. The bubbles were generally not spherical and their locations were not axially symmetric. The Rupert's drops thus prepared showed strength characteristics similar to those found by previous investigators. That is, if a

Fig. 4

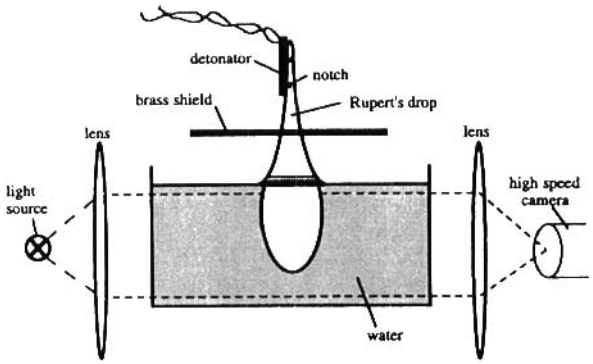

Schematic diagram of the experimental arrangement used for photographing the explosive disintegration of Rupert's drops. The water tank has transparent walls and several of the experiments were conducted with no water in the tank. Note the diagram is not drawn to scale.

blunt hammer was struck hard on the head of a drop, it would not break; on the other hand, if its tail was broken the whole drop would disintegrate immediately. When the drops were reheated beyond the softening temperature, the bubbles within them closed up, which suggested that they were pure voids or contained gases at very low pressures.

Several series of experiments were conducted to elucidate the mechanism of the explosive disintegration of Rupert's drops. In one, high-speed photography, working at a framing rate of $0{\cdot}5 \times 10^6$ frames s^{-1}, was employed to visualize the mode of fracture in the test drop and to measure the velocity of propagation of the crack front. A schematic diagram of the experimental arrangement used is shown in fig. 4. As it is known that when the tail of a drop is broken the entire drop disintegrates very rapidly, the initiation of cracking of the tail needed to be carried out to within an accuracy of 1 μs. This was achieved by rapidly exploding a small (26 mg) charge of lead azide placed on the tail at a point where it had been scribed with a sharp diamond tip. The lead azide charge was exploded rapidly by discharging a capacitor bank (applied voltage = 5 kV; total stored energy = 37 J) through a piece of bridge wire in contact with it. The fracture of the tail was always immediately followed by the disintegration of the entire drop. The event was back lit with the flash (duration = 80 μs) from a xenon-filled discharge lamp supplied by Q-arc (UK). The total discharge energy through the lamp was 60 J and the electrodes' potential difference was 1·5 kV. The entire fragmentation process was photographed with a Beckman and Whitley model 189 rotating-mirror framing camera working at a framing rate of $0{\cdot}5 \times 10^6$ frames s^{-1}. At this framing rate the exposure time per frame was 0·4 μs. The photographic film used was Ilford HP5 (400 ASA) and the magnification on it was 1 ×. The explosion of the detonator, the triggering of the flash lamp, and the relative position of the rotating mirror were synchronized electronically. To prevent the products of explosion of the detonator from obscuring the field of view, a 25 mm diameter brass shield was placed between the detonator and the head of the test drop, as shown in fig. 4. The crack front velocities were measured from the photographic prints and the accuracy of the measurements was about 7%.

In the second series, to visualize any stress waves generated by a disintegrating drop, the head of the drop was immersed under water contained in a transparent rectangular parallelepiped box made of perspex, while its tail remained out of the water. As before, a detonator was attached to the tail and the entire event was photographed in

Fig. 5

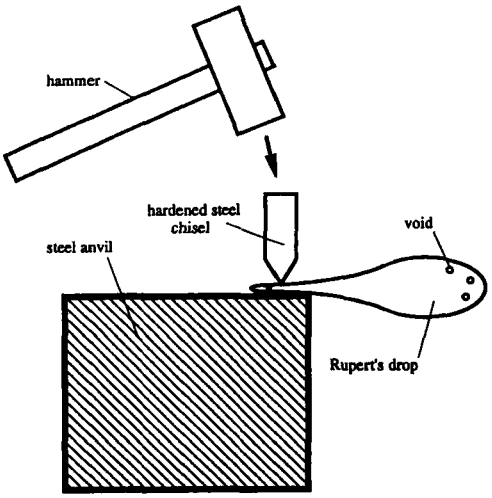

Schematic diagram of the experimental arrangement used for measuring the velocities of fragments of a disintegrating Rupert's drop.

transmission using high-sensitivity shadowgraphy. Previously, such an arrangement had been successfully used in visualizing 100 MPa shock waves in water (Bowden and Chaudhri 1968). In the third series, we investigated by means of high-speed photography the fracture behaviour of Rupert's drops which had been annealed by heating them at 530°C in air for 2 h and subsequently allowing them to cool down to room temperature over a period of 1·5 h. This is a standard annealing cycle for soda-lime glass and it relieves all the internal stresses and strains.

To determine the velocities of fragments of a disintegrating Rupert's drop, in the final series of high-speed photographic experiments a framing rate of only 6500 frames s^{-1} was used and the camera employed was a rotating-prism type (Hadland Hyspeed). The experimental arrangement used is shown schematically in fig. 5. Here the tail of the test drop was fractured with the impact of a hammer on to a hardened steel chisel resting on the tail, as shown in the figure. The fragmentation process was photographed in transmission over a period of 200 ms using the light from two 500 W electric light bulbs.

In other experiments, fragments of three Rupert's drops were examined under a scanning electron microscope (Cambridge Instruments, SEM 250) to characterize their sizes and surface morphologies. Also, a few drops were mounted in transparent epoxy, but with their tails remaining outside the epoxy. This method of encasement is quite similar to that used by Hooke (1665). The tails of the drops were then broken with finger pressure, which resulted in the total disintegration of the drops. However, the epoxy managed to keep the fragments in position so that the original shape of the drops was preserved. In a similar experiment, a piece of adhesive tape was wrapped around a Rupert's drop, having a head 6 mm in diameter. The tail was then broken with finger pressure, which caused the disintegration of the entire drop. The force of the disintegration was so severe that it removed cleanly a 5 mm diameter part of the tape at the head region; some fragments were also ejected from the drop through this punctured hole. However, the rest of the tape remained intact and preserved the fragments in position. Interestingly, through the punctured hole in the tape, it could be

seen under an optical microscope that some of the fragments remained stuck to the tape in their original positions. These fragments were examined under another scanning electron microscope (Electro Scan, Model E3). Fragments lying at the centre of the drop's head could also be examined through the hole in the tape.

The residual compressive stresses in the surface of the hemispherical heads of the drops were determined using an indentation technique (Chaudhri and Phillips 1990). Twenty-one drops were indented with a Vickers diamond indenter under a load of 49 N using a hardness testing machine (Leco Corporation). Before making indentations on a drop, it was suitably mounted. Then a flat of diameter of ~ 1 mm was made on its head by polishing it with very fine diamond grit. In a typical test, the maximum indentation load was reached in 15–25 s and the load was maintained for a period of 15 s before unloading. In six out of the 21 drops, median/radial cracks formed; the lengths of the surface traces of the cracks were measured under an optical microscope. In the remaining drops, surface chipping around the indentations occurred. The extent of the radial cracks was used in estimating the surface compressive stresses in the drops. To determine the thickness of the surface compressive layer of a drop's head, a Vickers diamond indenter was loaded on to it using a mechanical testing machine (Instron model 4502-001). The load was increased from zero using a cross-head speed of 0·25 mm min^{-1} until the drop failed catastrophically. The load at failure was recorded. In this manner, three Rupert's drops were examined. From such load measurements, the thickness of the compressive layer was estimated, as shown below (see § 3.8).

§ 3. Results and analysis

3.1. *Crack front velocity in Rupert's drops*

The high-speed photography was able to show clearly the propagation of the crack front within the Rupert's drops and their subsequent disintegration into numerous fragments. Figure 6 shows 8 consecutive frames from a typical high-speed photographic sequence. The intact body of the drop containing three bubbles (see arrow) is shown in frame 1. The explosion of the detonator occurs between frames 1 and 2, which probably initiated the fracture of the drop just where the detonator was placed on the tail of the drop (out of field of view of frame 1). The crack front in the drop emerges into the field of view in frame 2 (see arrow); the reaction products of the detonator can also be seen at the arrow labelled 'r'. (In the majority of such photographic experiments these products were kept outside the field of view by the brass shield.) Between frames 2 and 7 the crack front moves across the full length of the drop, and in every frame the position of the front is shown with an arrow. Note that the propagation velocity of the crack front is much higher than that of the reaction products of the detonator and therefore there was no difficulty in resolving fairly accurately the position of the crack front. Note also that as the drop has been back lit, the cracked zone appears dark. Moreover, as shown below, the fractured zone may consist of numerous small cracks. Therefore, individual cracks at the crack front could not always be resolved. However, occasionally, an individual bifurcating crack could be resolved at the main crack front. An example of such a crack can be seen at the arrow in frame 4. Such bifurcation and associated 'finger-type' cracks have also been observed in thermally tempered soda-lime glass blocks in which cracking was initiated by the impact of 2 mm diameter tungsten carbide spheres travelling at 150 ms s^{-1} (Chaudhri and Liangyi 1986). The presence of the bubbles in the glass drop does not appear to have any significant effect on the propagation pattern of the crack front. When the crack front reaches the exterior

Fig. 6

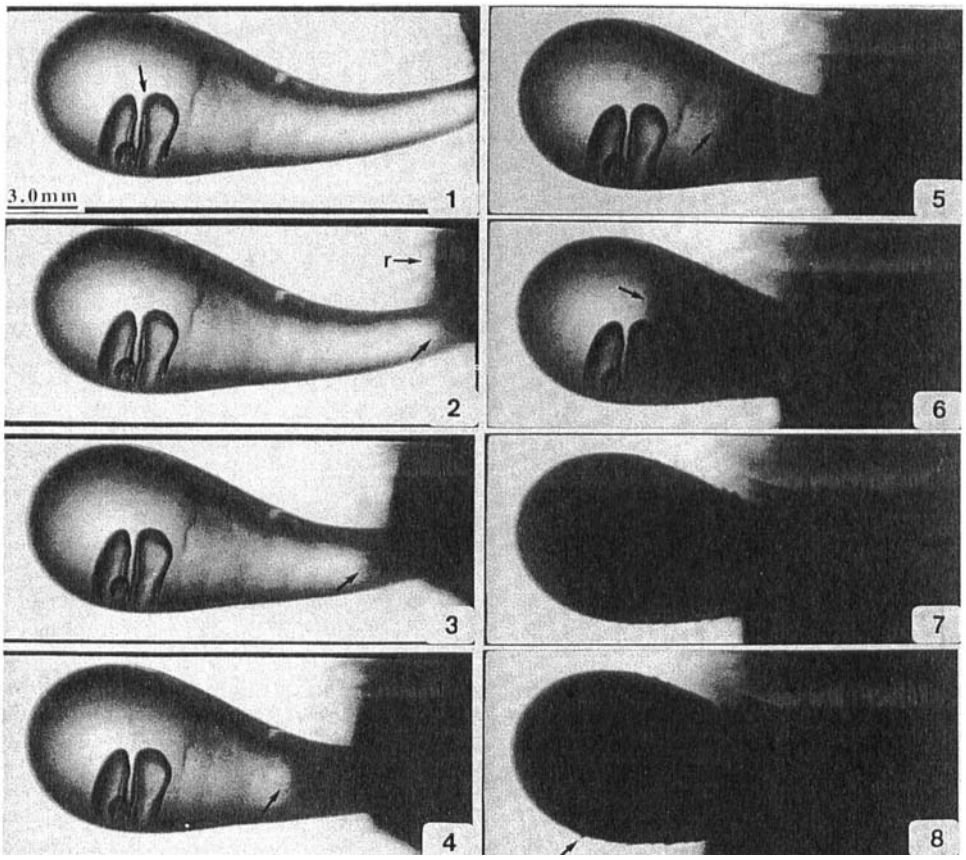

High-speed photographic sequence of the disintegration of a Rupert's drop. The voids in the drop are shown by the arrow in frame 1. The arrows in frames 2–6 mark the position of the disintegration front. In frame 2 the label 'r' indicates the front of the reaction products of the detonator. Interframe time = 2 μs.

surface of the drop, small fragments of the glass begin to be ejected from its surface (see arrow in frame 8). This causes the profile of the surface of the drop in frames 7 and 8 to become somewhat diffuse and irregular (see also figs. 7 and 8 below).

From measurements of the distance travelled by the crack front between successive frames (inter-frame interval = 2 μs), we have estimated its velocity in the glass drop. The crack front velocity was reasonably constant between frames 2 and 5 and between frames 5 and 7, with values of approximately 1630 and 1900 ms $^{-1}$, respectively. These values are close to the measured velocities of 1800 ms $^{-1}$ for self-propagating cracks in thermally tempered soda-lime glass blocks (Chaudhri and Liangyi 1986).

The bifurcation of the self-propagating cracks and the formation of the finger-type cracks can be seen more clearly in another high-speed photographic sequence, shown in fig. 7, of the disintegration of a glass drop; also note that this drop shows some surface rumplings of the type mentioned by Hooke (1665) and by de Luynes (1873). Here, the arrow at S shows the brass shield and the explosion of the detonator takes place in frame 1. The crack front can be seen in frame 2 at the arrow labelled C. Several finger-type

Fig. 7

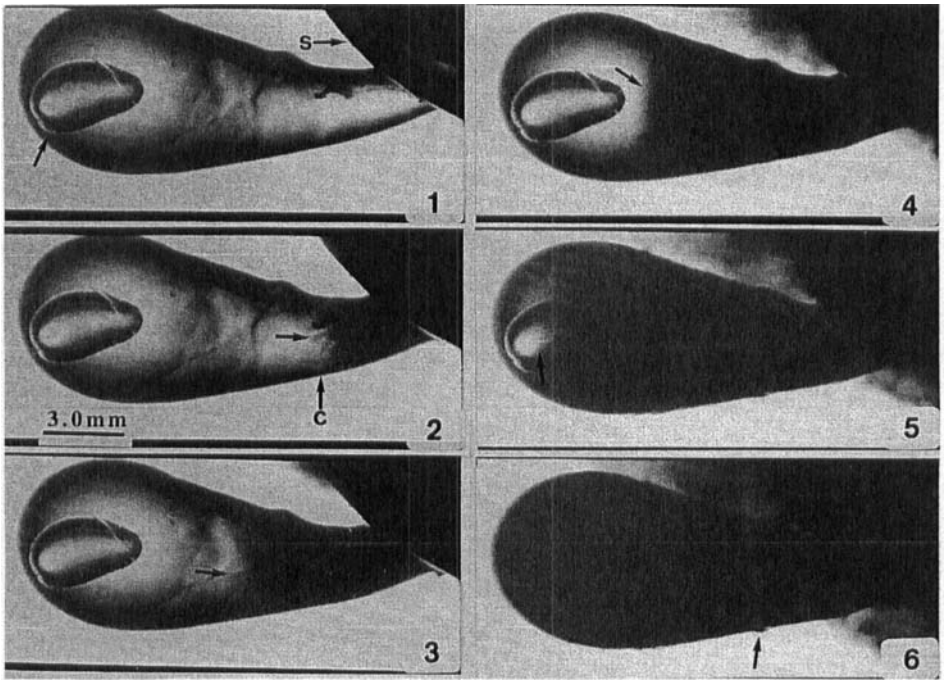

High-speed photographic sequence of the disintegration of a Rupert's drop in which the bifurcation events at the crack front can be seen quite clearly at locations given by the arrows in frame 2, 3 and 5. The brass shield S and a void inside the drop are shown by the arrows in frame 1. Interframe time = 2 μs.

cracks, formed by the bifurcation at the main crack front, can be seen at the arrows in frames 2, 3 and 5. They appear to extend ahead of the main crack front in these frames, but are contiguous with it. Small fragments from the fractured drop can be seen leaving its surface in frame 6 (see arrow) when the crack has propagated across the whole body of the drop. From measurements of the distances travelled by the crack front, we have estimated the front's velocity as being 1750 m s^{-1} between frames 1 and 2, 1565 m s^{-1} between frames 2 and 3, 1500 m s^{-1} between frames 3 and 4, and 1690 m s^{-1} between frames 4 and 5. These velocity values are similar to those measured from the photographic sequence shown in fig. 6. Measurements of crack front velocities from other high-speed photographic sequences of the fracture of 15 Rupert's drops in air generally gave values in the range 1450–1900 m s^{-1}. In all these experiments, the crack front velocities were reasonably constant within the tension zone of the drop.

It must be noted from figs. 6 and 7 that the crack front propagated quite uniformly from near the tail section (where it was initiated) towards the head of the drop. No other cracking, physically separate from the main front, was seen to occur.

3.2. *Fragment velocities*

Figure 8 is an immediate continuation of the photographic sequence of the fracture shown in fig. 7. The ejection of the fragments from the drop's surface is shown by the arrows in frames 1 to 6. From the displacements of the individual fragments in these frames, we have estimated their velocities to be in the range 10–20 ms^{-1}. It can be seen

Fig. 8

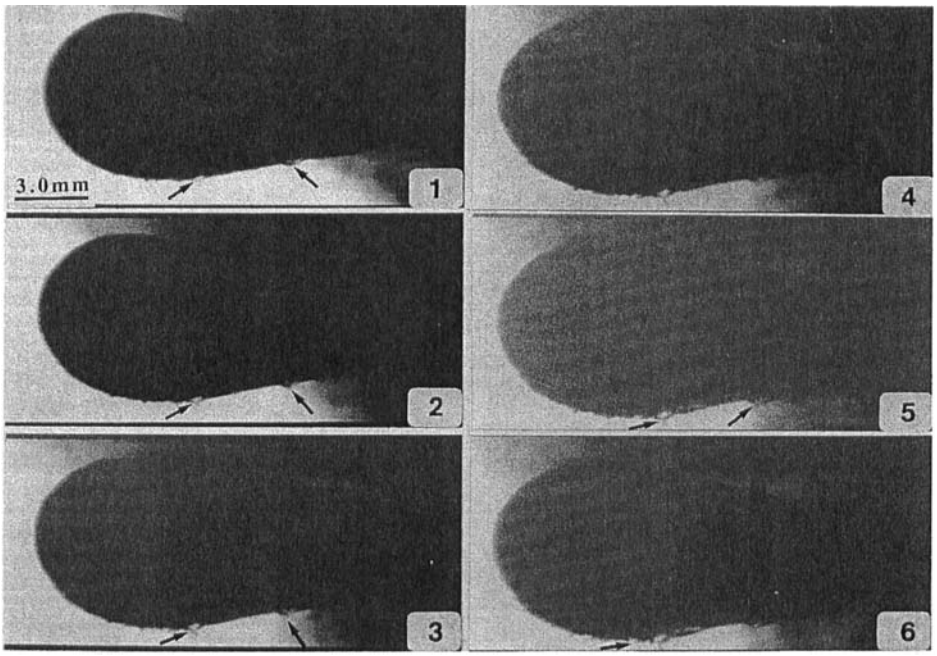

Immediate continuation of the sequence of photographs shown in fig. 7. The fragments leaving the surface are shown by the arrows.

in the sequences shown in figs. 6 and 7 that the transparency of the surface layer of the glass drops was quite poor. We were, therefore, unable to determine the velocities of the cracks through this surface layer. It is very likely, however, that as the cracks travel to the drops' surface through the compression zone, their velocities are very much reduced. This suggestion is based on the high-speed photographic observations of the disintegration of thermally tempered rectangular parallelepiped blocks of soda-lime glass (Chaudhri and Liangyi 1986). These authors found that the velocities of the cracks practically dropped to zero as the cracks entered the surface compression zone.

In order to obtain estimates of the fragment velocities over longer time durations (i.e., 200 ms), high-speed photographic investigations of the fracture of Rupert's drops were made at a slower framing rate of 6500 frames s^{-1} using the rotating-prism camera (Hadland Hyspeed). Frames 1–4 of fig. 9 show a few selected frames from a typical photographic sequence, taken with transmitted light, of the fracture of a Rupert's drop. In this experiment, a fracture was initiated by impacting a hardened steel chisel edge (see arrow e, frame 1) on to the tail region of the drop which was placed on a steel anvil (see arrow a, frame 1). It can be seen that the crack propagated through the entire drop in 0·15 ms (frame 2), and the fragments of the disintegrated drop can also be seen leaving the surface in this frame (see arrows; the fuzziness has been caused by the relatively long exposure time). The displacement of the fragments leaving the surface of the drop is seen to be spherically symmetric over a time duration of ~ 200 ms, (see frames 3 and 4). From measurements of the displacements of the individual fragments and the expansion of their envelope (see arrows) in frames 2–4 and subsequent frames, we estimated the fragment velocities to be in the range 0–25 m s^{-1}. It is reasonable to

Fig. 9

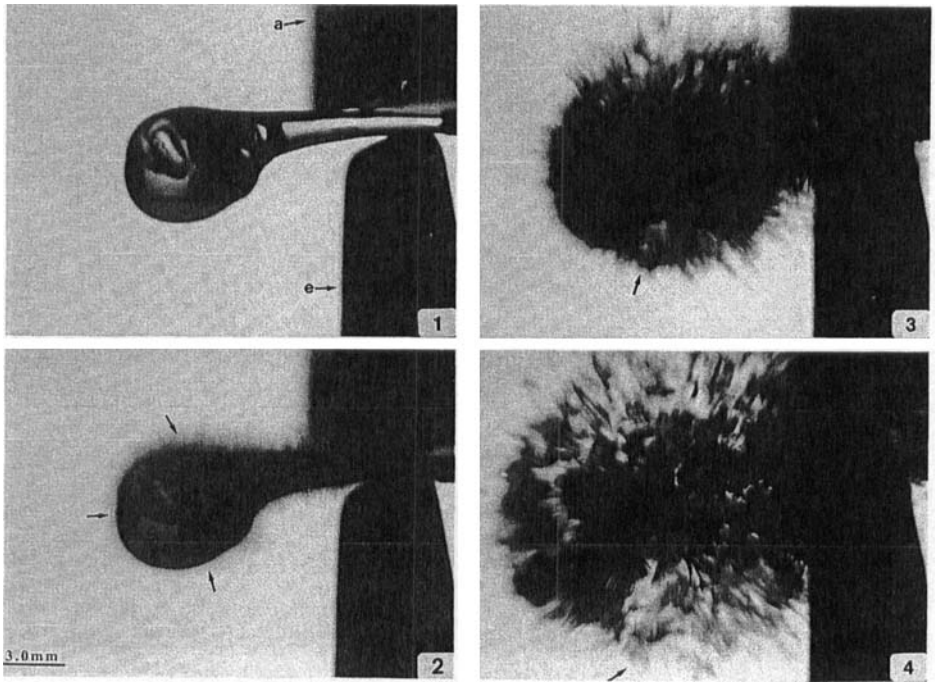

A typical high-speed photographic sequence of the disintegration of a Rupert's drop taken with a rotating prism camera (Hadland Hyspeed). The drop rests on a steel anvil a and a hardened steel chisel e (frame 1) impacts the tail of the drop between frames 1 and 2, which leads to the disintegration of the entire drop. Frames 2–4 show the spreading of the fragments, their velocities being as high as 25 ms^{-1}. Interframe time = 0·15 ms.

assume, because of the surface compression, that the fragments originating at the centre of the drop will have higher velocities than those at the surface.

3.3. *Similarities with cracking in thermally tempered glass*

The majority of the crack propagation features seen in a disintegrating Rupert's drop are similar to those observed from catastrophically disintegrating thermally tempered soda-lime glass blocks. Figure 10 is a high-speed photographic sequence from the paper by Chaudhri and Liangyi (1986), showing the catastrophic failure of a thermally tempered soda-lime glass block caused by the impact of a 2 mm diameter tungsten carbide sphere travelling at a velocity of 150 $m\,s^{-1}$. The fringes in frames 1–4 are isochromatics and the arrow in frame 1 indicates the black fringe which marks the region of zero stress—the boundary between the tension and compression zones. The velocity of the cracks is at least 1000 $m\,s^{-1}$ between frames 2 and 3, and 1500 $m\,s^{-1}$ between frames 4 and 5. In other sequences from that study, crack velocities as high as 1800 $m\,s^{-1}$ were measured, which are close to our measured crack velocities in the Rupert's drops. Between frames 4 and 5, the cracks enter the tension zone and this leads to the initiation of the catastrophic failure of the block. In the tension zone the cracks spread at a speed of $\sim 1500\,m\,s^{-1}$. However, in the compression zone (i.e., adjacent to the impact surface), the crack propagation speed is only ~ 200–$300\,m\,s^{-1}$, possibly reducing to zero as the cracks approach the surface (see frames 6–12). Also, in frames

Fig. 10

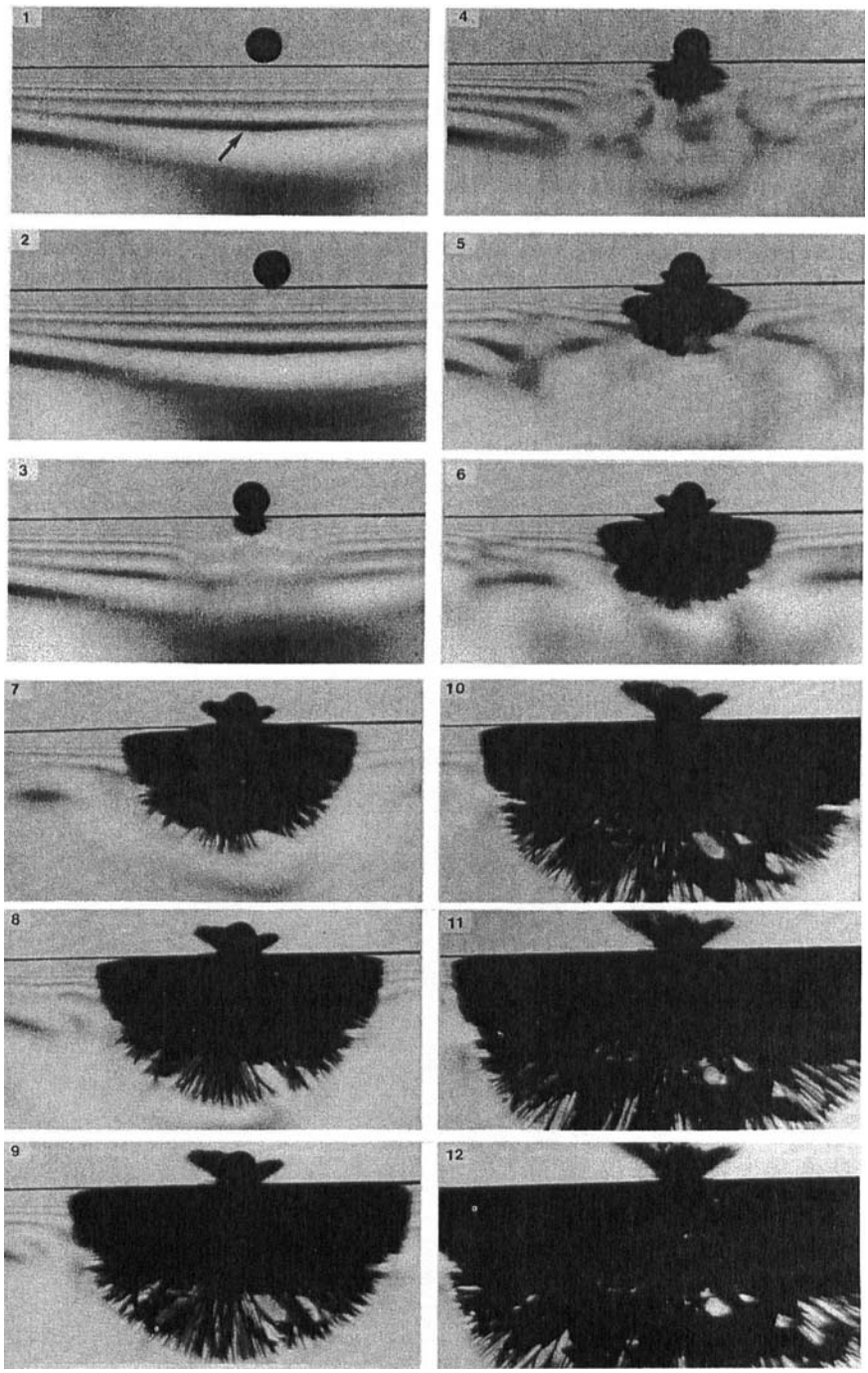

High-speed photographic sequence showing the catastrophic failure of a thermally tempered glass block caused by the impact of a 2 mm diameter tungsten carbide sphere at a velocity of 150 ms^{-1}. The fringes are isochromatics; the arrow points to the black fringe, which marks the region of zero stress. The catastrophic failure begins in frame 4. Surface compressive stresses = 200 MPa, interframe time = 1 μs, loading time of the impact cycle = 3·5 μs. Frames 7–12 are the continuation of the sequence shown in frames 1–6. Note the bifurcation of the cracks in frames 7–12. From Chaudhri and Liangyi (1986).

7–12, crack bifurcation at the crack front can be seen clearly. This bifurcation appears to be similar to that observed by us in the Rupert's drops. A further point to note from the isochromatics in frames 4–9 is that as the size of the disintegrated zone grows, the stress state appears to change just ahead of the disintegration front. However, no cracks are initiated at sites which are physically separated from the disintegration front.

3.4. *Fracture of annealed glass drops*

As would be expected, annealed Rupert's drops did not disintegrate catastrophically when their tails were fractured. A typical high-speed photographic sequence is shown in fig. 11. The explosion of the detonator occurs 2 μs prior to frame 1 and the first fractures will be seen in frame 2 at positions shown by the arrows. The head of the drop separates from the tail along the crack shown by the arrow in frame 6 and a large part

Fig. 11

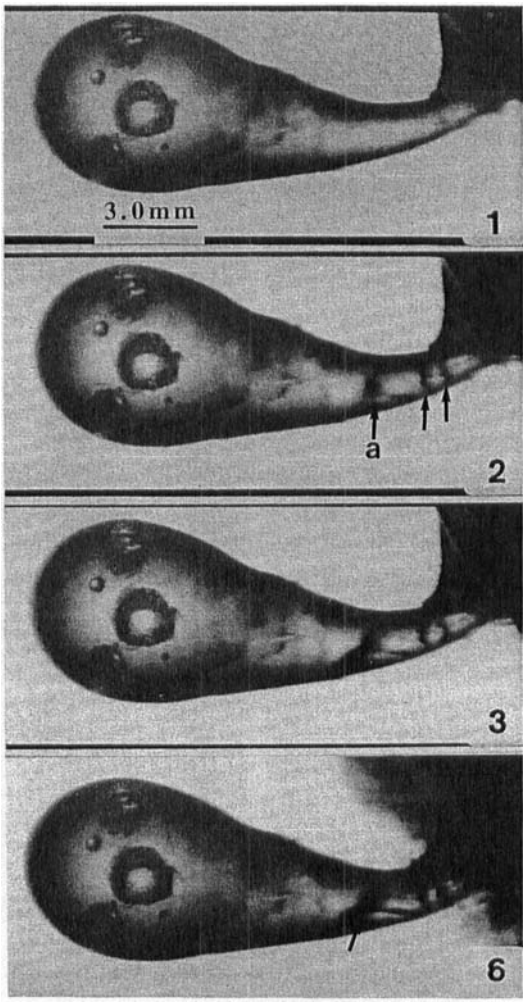

High-speed photographic sequence of an annealed Rupert's drop which failed to disintegrate catastrophically when its tail was broken. The bubble-like features on the drop are surface deposits. Interframe time = 2 μs.

of the drop, about 6 mm in diameter and 10 mm in length, was recovered intact along with most of the tail.

3.5. *Stress wave visualization*

In order to determine whether any significantly strong stress waves were generated during the fracture of Rupert's drops, Schlieren photography was carried out on the disintegrating drops whose heads were immersed in water, with their tails remaining outside of it. As before, the tail of the test drop was broken with the explosion of a detonator. Figure 12 shows a typical high-speed photographic sequence. The detonator exploded 4 μs before frame 1 and the crack front in the drop can be seen entering the field of view in frame 2 (see arrow). The crack front has propagated throughout the hemispherical head of the drop by frame 4. From frames 2 and 3 the crack front velocity is estimated to be at least 975 m s^{-1}, while the velocity of the fragments leaving the

Fig. 12

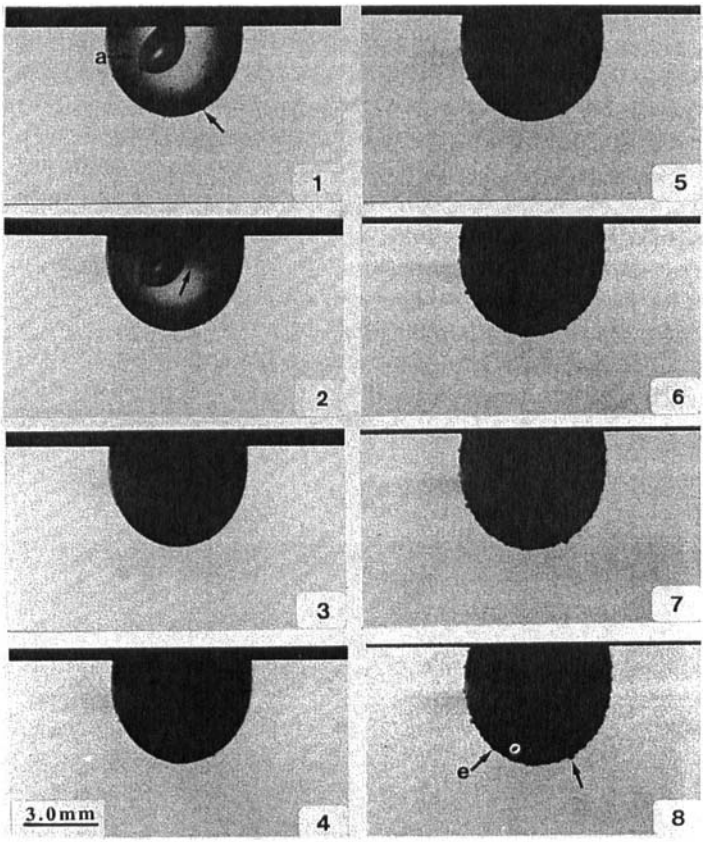

High-speed photographic sequence of the disintegration of a Rupert's drop whose head is immersed in water but whose tail is outside it. In frame 1 a void within the drop is shown at a and the unlabelled arrow shows a small air bubble, which is attached to the drop's surface. The tail of the drop was broken 4 μs before frame 1 and the disintegration front inside the drop is shown by the arrow in frame 2. By frame 3, the entire drop has disintegrated and a fragment is seen detaching from the drop's surface at e in frame 8. No stress waves appear to be transmitted from the drop to the water and even the air bubble attached to the drop's surface is not disturbed (see the unlabelled arrow in frame 8). Interframe time = 2 μs.

surface of the drop is about 12–15 $m\,s^{-1}$ (frames 5 to 8). A careful examination of frames 1–8 shows that no shock waves appear to be transmitted to the water. It is interesting to observe from fig. 12 that even the small air bubbles which had migrated from the water and attached themselves to the drop surface before disintegration of the drop (such as the one shown by the arrow in frame 1) do not appear to have been perturbed by any stress waves from the disintegrating drop (see arrow in frame 8). Also, as shown by the arrow in frame 8, a fragment can be seen just forming at the drop's surface. This photographic sequence conclusively demonstrates that the coupling of the stress waves generated by the detonator to the main body of the drop is relatively weak, and that the strength of any stress waves due to the drop's disintegration is also insignificant.

3.6. *Scanning electron microscopy observations of fragments*

Figures 13 (*a*)–(*c*) are typical scanning electron micrographs of some of the fragments, which were collected after the disintegration of three Rupert's drops. Most of the fragments are thin platelets (fig. 13 (*a*)), while a few are needle-shaped splinters. Figure 13 (*b*) shows a typical fracture surface of a thin platelet-type fragment, whose surface appears to be very smooth though a few smaller fragments can be seen lying on it. However, the lower left-hand part of the fracture surface has several striations, which are clearly visible in the higher magnification micrograph shown in fig. 13 (*c*). The origin of these striations is at present not clear. Also, some fragments have conchoidal fracture surfaces. Since the fragments were produced by very high velocity cracks, it is especially interesting to note that so many of the fragments had very smooth surfaces. This would suggest that a very smooth fracture surface does not necessarily mean that the fracture was produced by a very slow speed crack. Similarly, hackles on a fracture surface are not definite indications of a high velocity crack.

We believe that the smallest fragments are generated within the inner zone of the drop in which the high tensile stresses had caused many bifurcation events. Though we did not examine a sufficiently large number of fragments to be able to determine a

Fig. 13

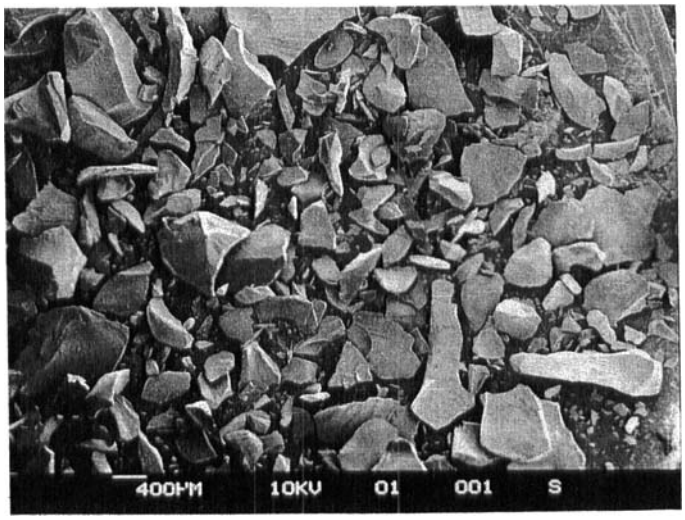

(*a*)

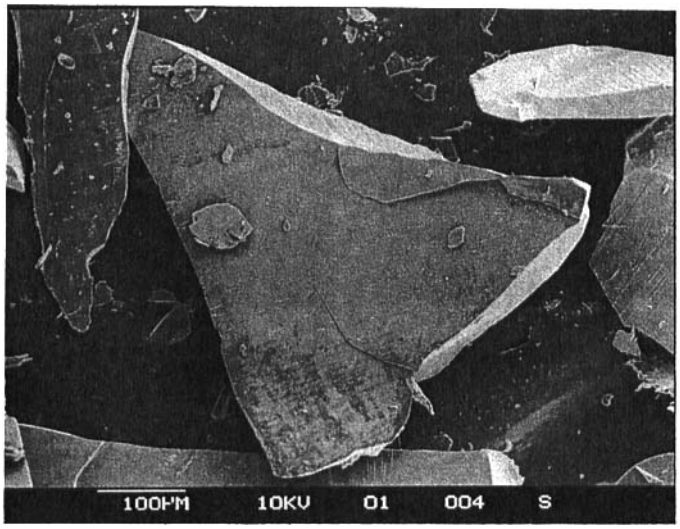

(*b*)

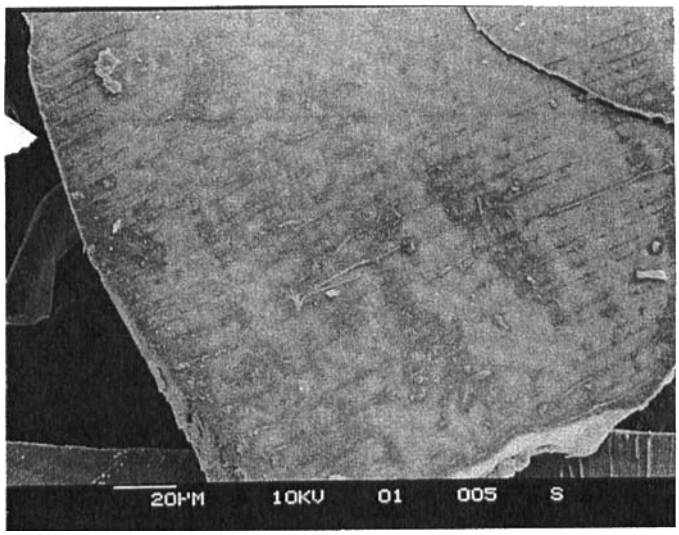

(*c*)

Scanning electron micrographs of the fragments of disintegrated Rupert's drops. A general view of the fragments is shown in (*a*); note that many fragments are plate-like and one such fragment is shown in (*b*). Most of the surface of the flat is smooth, but at the bottom corner there are striations, which can be seen more clearly in (*c*).

statistical distribution of their sizes, we could estimate the mean size of the large (largest dimension $\geqslant 0{\cdot}5$ mm) and small (largest dimension $\leqslant 200\,\mu$m) fragments. The mean size of the large fragments was $\sim 1{\cdot}3$ mm, whereas that of the small particles was $\sim 110\,\mu$m. The largest measured particle size was $\sim 2{\cdot}3$ mm, while the smallest was $\sim 15\,\mu$m.

From the sizes of the fragments recovered, it is possible to make an estimate of the maximum tensile residual stresses existing within the interiors of the Rupert's drops.

Fig. 14

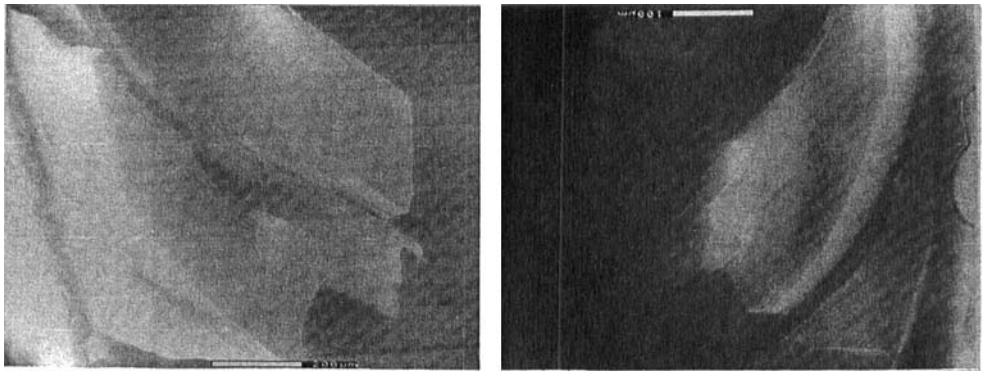

(*a*) (*b*)

Scanning electron micrographs of two sets of *in situ* fragments of a disintegrated Rupert's drop. These sets were from the two ends of a diameter, at right angles to the drop's axis, of the drop's head and were kept in position by wrapping the intact drop in a piece of adhesive tape and then causing the disintegration by breaking its tail. The fragments shown in (*a*) and (*b*) are from the left and right hand sides, respectively, of the drop's head and the tail of the drop is towards the bottom of the page. In each set, the fragments are parallel to one another, and close to the drop's surface the fracture surfaces appear to run parallel to it.

It has been stated by Holloway (1973) that the distance t between two successive bifurcation points along a crack path depends on the magnitude of the maximum tensile stress σ_t in the glass. This dependence is given by

$$\sigma_t^2 t = \text{constant}, \tag{1}$$

where the constant has a value of $4 \times 10^{11}\ \mathrm{N^2\,m^{-3}}$ for soda-lime glass. It is fair to assume that the fragment size is, to a reasonable approximation, equal to the bifurcation distance and that the smaller fragments are generated within the tensile zone. Therefore, for the smallest fragment size of 15 μm, the estimated tensile stress σ_t comes out to be 160 MPa.

Figures 14 (*a*), (*b*) show scanning electron micrographs of the fragments of a disintegrated drop, which are from the surface region of the drop's head and which were preserved in their positions by a piece of adhesive tape. The fragments shown in fig. 14 (*a*) were at one end of a diameter, normal to the direction of crack propagation, of the drop's head, whereas those shown in fig. 14 (*b*) were from the opposite end of the diameter. Note that each set of fragments consists of plates lying almost parallel to one another and inclined to the drop's axis. However, the fragments indicate that the cracks' surface became approximately parallel to the drop's surface as they reached it. We have previously reported similar observations from the catastrophic failure of thermally tempered blocks of soda-lime glass (Chaudhri and Liangyi 1986). We therefore suggest that the surface compressive stresses in the drop's head constrain the cracks to run parallel to its surface.

3.7. *Absence of conical fragments*

The high-speed photographic sequence shown in figure 9 gives no evidence for the existence of conical fragments in a disintegrating drop, such as those reported by Moray (see Merrett (1662)) and by de Luynes (1873). Neither do the scanning electron

micrographs shown in figures 13 and 14 give any support to the idea of the existence of conical fragments.

3.8. *Residual stress determination*

The surface compressive stress in a Rupert's drop was determined from measurements of the extent of the surface traces of the radial/median cracks formed due to indentations by a Vickers diamond pyramid under a load of 49 N. The relationship used is that given by Chaudhri and Phillips (1990). That is,

$$\sigma_c = \frac{\chi(P_n^* - P_n)}{1{\cdot}16c_n^2}, \tag{2}$$

where P_n^* and P_n are the loads which produce cracks of radius c_n in both the tempered and the annealed glass, respectively, $K_{IC} = 0{\cdot}75\,\text{MPa}\,\text{m}^{1/2}$, $\chi = 0{\cdot}0725$, and σ_c is the compressive stress in the drop's surface. The values of the compressive stresses thus determined are shown in table 1 and they are in the range 90–170 MPa.

By measuring the loads at which the Rupert's drops failed catastrophically when loaded with a Vickers indenter, we have been able to determine approximately the thicknesses of the surface compressive zone of the drops. Table 2 gives the measured loads at which the catastrophic failure of three drops occurred. Based on the assumption that the drops will fail catastrophically when the depth c of a median crack produced by the Vickers indenter just exceeds the thickness d_c of the compressive zone, and that the value of σ_c in these drops is 125 MPa, the values of d_c were calculated; these are in the range of 0·9–1·05 mm (see table 2). It will be seen from table 2 that the compression zone thickness is about 13% of the diameter of a drop's head. The mean thickness of the compression zone is 0·9 mm and it is interesting that this compares well

Table 1. Compressive residual stress σ_c in the surface of Rupert's drops. Mean value of $\sigma_c = 125$ MPa.

Head diameter d (mm)	Indentation load (N)	Measured crack length (mm)	σ_c (MPa)
5·6	49	0·146	92
7·2	49	0·130	126
6·7	49	0·120	154
7·6	49	0·116	168
8·9	49	0·140	102
6·5	49	0·137	108

Table 2. Estimated thickness d_c of the compressively stressed surface layer in Rupert's drops. Mean value of the compressive surface layer $d_c = 0{\cdot}9$ mm.

Drop diameter D (mm)	Indentation load at fracture, P (N)	d_c (mm)
6·4	1880	0·9
7·9	2550	1·05
7·2	1725	0·86

with the mean size of $\sim 1{\cdot}3$ mm for the larger fragments (see § 3.6). This supports our suggestion that the largest fragments are produced in the compression zone of the drops.

§ 4. Discussion

Our experimental observations and measurements have yielded a considerable amount of new information about the processes occurring during the explosive disintegration of Rupert's drops, the size, shape and surface morphologies of their fragments, and the magnitudes of the compressive stresses within the surface of intact drops and the tensile stresses at their centres. We shall discuss these results separately.

4.1. *The mode of fracture and the crack front velocity*

The high-speed photographic sequences of the disintegration process showed that when a crack was initiated in the tail of a drop, a crack front propagated at approximately the maximum velocity from the point of initiation towards the head of the drop. The crack front was self-propagating and was driven by the stored elastic energy within the drop. From several photographic sequences, the crack front velocity was measured as 1450–1900 m s^{-1}.

The high-speed photographic sequences also showed that the cracks, initiated in the tail of the drop, bifurcated repeatedly as they propagated in the tensile zone; the bifurcations gave rise to finger-type cracks which were sometimes seen to extend ahead of the crack front (see, for example, frames 2, 3 and 5 of fig. 7). The finger-type cracks were, however, part of the main crack front. Furthermore, the bifurcation of the cracks did not appear to slow down the main crack front. This type of crack propagation and associated bifurcation occurring within the tensile zone of the drops is very similar to that observed from self-propagating cracks in the tempered soda-lime glass blocks (see fig. 10). It may be added that in none of the 15 photographic sequences of the fracture of the Rupert's drops did we observe any secondary cracking taking place at a point which was physically separated from the main crack front. The crack velocities of 1450–1900 m s^{-1} observed in the present experiments are close to the measured velocities of self-propagating cracks in thermally tempered soda-lime glass blocks (Chaudhri and Liangyi 1986). Crack velocities of up to 1550 m s^{-1} have also been observed in stress-free soda-lime glass blocks (Chaudhri and Walley 1978). Our measured maximum crack velocities are significantly higher than the upper limit of 1500 m s^{-1} for the crack velocity in soda-lime glass as given by Schardin (1959). Schardin pointed out that this limit depended on the composition of the glass. We did not record crack velocities in excess of 1900 m s^{-1} in any of our experiments with the Rupert's drops.

Observations of self-propagating cracks (initiated by impact) in thermally tempered blocks have revealed (Chaudhri and Liangyi 1986) that the cracks slow down dramatically from 1500 m s^{-1} to about 200–300 m s^{-1} as they enter the surface layers of the blocks containing compressive residual stresses. The surface curvature of the Rupert's drops made it difficult to measure the crack velocities within their surface layers. However, we believe that it is most likely that in this case also the crack velocity decreases very dramatically as the cracks enter the compression zone of the drops.

The photographic sequence shown in fig. 12 clearly gives no evidence of the production of any sufficiently strong stress waves due to a fast moving crack front. If

there were such waves, they should have been transmitted to the surrounding water and would have been clearly visible in the shadowgraphs. (Such a high-speed shadowgraph system is capable of revealing shock waves in water of the strength of 100 MPa and more (Bowden and Chaudhri 1968).) Moreover, in none of the 15 high-speed photographic sequences of the disintegrating drops did we see any evidence of the initiation of new fracture sites, which were physically separated from the crack front. All these observations would rule out the stress wave focusing mechanism for disintegration of the drops, which was proposed by Johnson and Chandrasekar (1992).

4.2. *Fragment sizes and surface morphologies*

The measurements made using the indentation technique showed that in our Rupert's drops the surface compressive stresses were in the range 90–170 MPa and that the mean thickness of the surface compressive layer of drops of head diameters 6·4–7·9 mm was estimated to be $\sim 0{\cdot}9$ mm. The interior of the drops is under tensile stresses, the maximum estimated value being ~ 160 MPa. It is these tensile stresses which drive the disintegration through the drop. The fragment sizes were in the range 15 μm to 2·3 mm, with the larger ones being in the form of thin plates.

We believe that the smallest-sized particles originate at the drop's centre, where the tensile stresses are maximum and the likelihood of crack bifurcation is highest. On the other hand, the largest particles are formed within the surface compressive zone. Moreover, in this zone the crack velocities will be much smaller, even approaching zero, and the process of bifurcation will be absent.

It is interesting to note that some of the fragments of Rupert's drops were found to have ejection velocities of up to 25 m s^{-1}. This observation is different from that made from the catastrophic failure of a rectangular parallelepiped block of thermally tempered soda-lime glass block which had similar surface compressive stresses. In this case the fragments were not ejected from the surface and in fact remained preserved in position by themselves. At present we are not able to explain fully these differences between the behaviour of a Rupert's drop and that of a block of thermally tempered soda-lime glass.

As already stated above, we were unable to find any evidence for conical fragments of a Rupert's drop, which Hooke (1665) imagined to exist, and which were experimentally observed by Moray (see Merrett (1662)) and by de Luynes (1873). If such fragments existed during the fragmentation of a Rupert's drop used in this work, we would have observed them in the high-speed photographic sequences taken at a moderate framing rate of 6500 frames s^{-1}. The scanning electron micrographs of the fragments (see figs. 13 and 14) do not indicate that they could possibly be part of conical pieces. There were, however, a few plate-like fragments found near the surface of a disintegrated drop, which indicated a preferential orientation. Perhaps the existence of such fragments may have given Moray (see Merrett (1662)) and de Luynes (1873) the idea of conical fragments.

4.3. *A model of the disintegration process*

Figure 15 (*a*) shows a schematic diagram of a drop, with the tension zone included within ABC and the compression zone lying between the surface ABC and outer boundary DEF of the drop. At a point near A, a crack is introduced in the tension zone by the explosion of a small amount of lead azide charge, the impact of a hardened steel chisel, or with finger pressure. Owing to the existence of high tensile stresses, the initial

Fig. 15

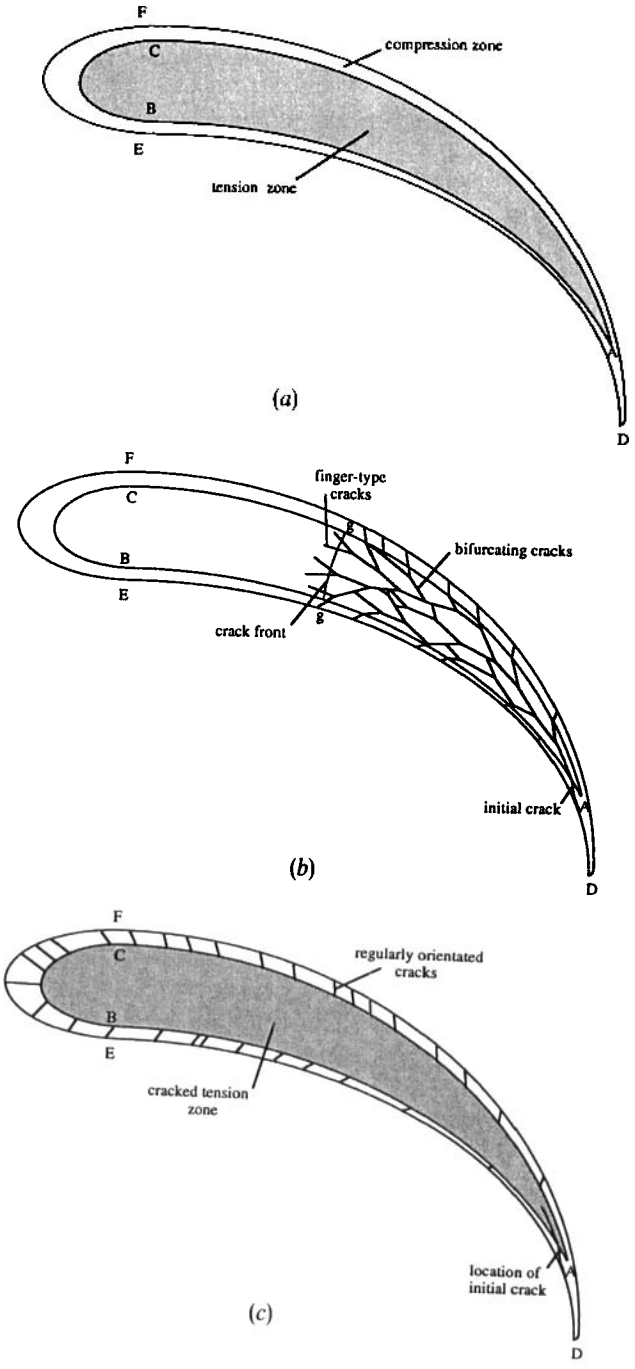

Schematic representations of the proposed model of the disintegration of a Rupert's drop. (*a*) The inner tension zone and the outer compression zone of a Rupert's drop. (*b*) An axial section of the disintegrating front travelling from the tail-end towards the head. (*c*) The completely disintegrated drop with regularly oriented cracks within the compression zone. Perhaps the existence of such cracks led Merrett (1662), Hooke (1665) and de Luynes (1873) to the idea of conical fragments.

crack accelerates rapidly to a high velocity and bifurcates. The forked cracks thus formed propagate some distance and bifurcate. This process of bifurcation continues till the entire drop has become fragmented. An intermediate stage is represented in fig. 15 (*b*), in which the crack front is represented by the line gg, where a bifurcation event causing the formation of finger-type cracks is also shown. Because of their momentum, fast cracks will penetrate into the compression zone, but their velocities will be very much reduced. In this region, there is no bifurcation, but the cracks are regularly oriented to the surface, as shown in fig. 15 (*c*). On a microscope level and very close to the external surface of the drop, these cracks tend to run almost parallel to the surface (see fig. 14). At present we do not have a clear understanding of the reasons for the inclination of the surface cracks. It will be noted from fig. 15 (*b*) that our model does not suggest the formation of conical fragments. When the entire drop has been disintegrated, but its fragments are preserved in position, it may appear as shown schematically in fig. 15 (*c*).

§ 5. Conclusions

The main achievement of these high-speed photographic investigations has been the ability to photograph the interior zone of a disintegrating Rupert's drop using transmitted light. In the photographic sequences, the features of fast-moving cracks in Rupert's drops have been clearly revealed. The velocity of the crack front has been found to be fairly constant within the interior tension zone and values in the range 1450–1900 m s^{-1} have been recorded. That is, the crack velocities were in the range 0·27–0·36 of the longitudinal wave velocity in the glass. At the crack front, bifurcation was also observed in several photographic sequences. Velocities of the fragments and their sizes were also measured. Moreover, it has been shown that a disintegrating drop does not produce any sufficiently strong stress waves, which may influence its fragmentation. Based on all these observations, a satisfactory and self-consistent mechanism for the explosive disintegration of a Rupert's drop has been proposed.

Acknowledgments

We would like to thank Dr E. H. Yoffe of the department of Materials Science and Metallurgy of this university for numerous discussions on the subject, for translating several of the papers cited in this work, and for valuable comments on the manuscript. We also thank Dr A. D. Yoffe of our laboratory for his interest and encouragement. One of us (S.C.) would like to thank Professor W. Johnson, F.R.S., for introducing him to the problem of Prince Rupert's drops and the US National Science Foundation for grant DDM-9057916 used in partial support of this work.

References

Bowden, F. P., and Chaudhri, M. M., 1968, *Nature*, **220,** 690.
Brodsley, L., Frank, C., and Steeds, J. W., 1986, *Notes Rec. R. Sec. Lond.*, **41,** 1.
Chandrasekar, S., and Chaudhri, M. M., 1993, *Phil. Mag.* A, **67,** 1187.
Chaudhri, M. M., and Liangyi, C., 1986, *Nature*, **320,** 48.
Chaudhri, M. M., and Phillips, M. A., 1990, *Phil. Mag.* A, **62,** 1.
Chaudhri, M. M., and Walley, S. M., 1978, *Phil. Mag.* A, **37,** 153.
Chaudhri, M. M., Wells, J. K., and Stephens, A., 1981, *Phil. Mag.* A, **43,** 643.
de Freminville, M. Ch., 1914, *Rev. de Metall.*, **11,** 971.
de la Bastie, F. B. A. R., 1874, *Tempering Glass*, British Patent no. 2783.
de Luynes, V., 1873, *Ann. Chim. Phys. 4 Serie.*, **30,** 289.
Harlin, G., and Jones, A. D. W., 1978, Third-year physics project theses (project no. 22, 1978; as quoted in Brodsley, Frank and Steeds (1986)).

HOLLOWAY, D. G., 1973, *The Physical Properties of Glass* (London: Wykeham), p. 188.
HOOKE, R., 1665, *Micrographia*, a facsimile edition (Lincolnwood: Science Heritage Ltd), pp. 33–44.
JOHNSON, W., and CHANDRASEKAR, S., 1992, *J. Mater. Process. Tech.*, **31**, 413.
LITTLETON, J. T., and PRESTON, F. W., 1929, *J. Soc. Glass Technol.*, **13**, 336.
MERRETT, C., 1662, *The Art of Glass* (London: Octavian Pulleyn), pp. 353–362.
PELIGOT, E., 1877, *Le Verre*, Editeur, G. Masson (Paris: Libraire De L'Academie De Medicine), pp. 24–32.
SCHARDIN, H., 1959, *Fracture*, edited by B. L. Averbach, D. K. Felbeck, G. T. Hahn and D. A. Thomas (London: Wiley), pp. 297–330.